Beslier, M.-O., Whitmarsh, R.B., Wallace, P.J., and Girardeau, J. (Eds.)
Proceedings of the Ocean Drilling Program, Scientific Results Volume 173

6. Data Report: Lithology and Microfacies of Late Cretaceous to Early Tertiary Turbidites from Sites 1068 and 1069[1]

Hans-Joachim Wallrabe-Adams[2]

ABSTRACT

Thin sections of samples were studied from (syn-?) postrift sediments of the Iberia Abyssal Plain (Ocean Drilling Program Leg 173, Sites 1068 and 1069). They show that, at these sites, Lower Cretaceous calcareous chalks and calcareous mass-flow deposits are overlain by sub-calcite compensation depth pelagic claystones of Late Cretaceous to early Tertiary age. At both sites, turbidites and current-controlled sequences are intercalated with pelagic claystones and show similar variations: (1) the proportion of turbidites to pelagic clay varies systematically and (2) turbidite composition changes from relatively coarse-grained and calcareous to predominantly fine-grained siliciclastic. This facies transition occurs around the Paleocene/Eocene boundary. In addition, turbidites at the Cretaceous/Tertiary and the Paleocene/Eocene boundaries contain resedimented glauconite, and, occasionally, some pyrite.

INTRODUCTION

During Ocean Drilling Program (ODP) Leg 173, five holes (1065A, 1067A, 1068A, 1069A, and 1070A) were drilled in the Iberia Abyssal Plain, completing a west-to-east transect of five previously drilled sites (ODP Leg 149). This transect runs perpendicular to the ocean–continent transition (OCT) zone at the western Iberian margin south of Galicia Bank (Fig. **F1**). Because the structural basement of the OCT zone

F1. Bathymetric chart of the western Iberian margin, p. 6.

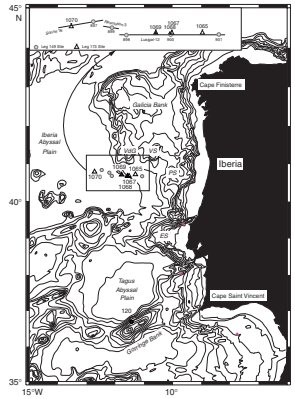

[1]Wallrabe-Adams, H.-J., 2001. Data report: Lithology and microfacies of Late Cretaceous to early Tertiary turbidites from Sites 1068 and 1069. *In* Beslier, M.-O., Whitmarsh, R.B., Wallace, P.J., and Girardeau, J. (Eds.), *Proc. ODP, Sci. Results*, 173, 1–11 [Online]. Available from World Wide Web: <http://www-odp.tamu.edu/publications/173_SR/VOLUME/CHAPTERS/SR173_06.PDF>. [Cited YYYY-MM-DD]
[2]Institute of Geosciences, Department of Geology, University of Kiel, Olshausenstrasse 40, D-24118 Kiel, Federal Republic of Germany.
hjwa@gpi.uni-kiel.de

Initial receipt: 26 October 1999
Acceptance: 18 November 2000
Web publication: 1 May 2001
Ms 173SR-013

(oceanic and continental crust) was the major target of Leg 173, the overlying sediments were cored only from ~150 m above the basement (ODP Leg 173 Shipboard Scientific Party, 1998). The cored (syn-?) postrift sediments range from Early Cretaceous to middle Eocene in age. Some older sediments (Jurassic) present belong to the continental prerift basement (Holes 1065A and 1069A). This report presents results of sedimentological analysis completed primarily on turbidites from Unit II of Sites 1068 and 1069.

METHODS

Samples were obtained from Upper Cretaceous to lower Tertiary turbidites or current-induced beds. Three to six samples were taken per core from Holes 1068A and 1069A.

Thin sections were made from all samples. They were investigated using a binocular petrographic microscope with a polarizing device for determining noncarbonate particles (maximum magnification = 40×). The percentage of particles and matrix/cement was estimated using visual composition diagrams.

The turbidites are intercalated between deep marine red-brown claystones (sub-calcite compensation depth [CCD]), which were also sampled, and from which W. Kuhnt and E. Urquhart analyzed benthic agglutinated foraminifers (Kuhnt and Urquhart, 2001).

RESULTS

At most sites (1068, 1069, and 1070) the continental or oceanic basement is overlain by marine calcareous mudstones (nannofossil oozes and chalks) ranging in age from Berriasian to early Valanginian (Hole 1069A), Valanginian to Barremian (Hole 1068A), and early to late Aptian (Hole 1070A). At Hole 1070A, these sediments are conformably overlain by an Upper Cretaceous sequence of yellow-red claystones, silty claystones, siltstones, and yellow-white sandstones (Unit III, Albian/Cenomanian–Paleocene) (Wallrabe-Adams et al., 1999; Kuhnt and Urquhart, 2001). The upper part of Unit III is comparable to the deep-sea claystones of the following Subunit IIC but lacks turbidites. All other sites show a hiatus up to the Campanian–Maastrichtian. The successive Maastrichtian to middle Eocene sequences in Holes 1067A–1070A consist of red-brown deep marine claystones (sub-CCD), which alternate with calcareous and siliciclastic turbidites, and bottom current-influenced deposits (contourites?). The facies development is best preserved at Sites 1068 and 1069, which therefore will be described in more detail. Significant parameters and results from Sites 1068 and 1069 are listed in Table T1.

T1. Petrographic features, Holes 1068A and 1069A, p. 9.

Dark red-brown pelagic claystones and the intercalated turbidites of Subunits IIB/IIC are arranged in decimeter-scale sequences that darken (become finer) upward. These begin with light-colored, relatively coarse-grained sediments (calcareous siltstone/sandstone, conglomerate) that become finer upward (calcareous silty claystone, sometimes nannofossil chalks) and grade into dark brown claystone. Often, bioturbation is marked by downward penetrating burrows filled with brown claystone. These sequences are strongly variable in thickness and lithologic development (see Shipboard Scientific Party, 1998a, p. 169, fig. 3).

Petrographic features of the samples are summarized in Table T1 and Figure F2. Details are provided below.

Site 1068

The marine sedimentary record at Site 1068 begins with coarse mass-flow deposits that enclose basement clasts (amphibolite, anorthosite, and metagabbro) and are deposited in a carbonate (chalk) matrix (lithologic Subunit IVA) (see Fig. F2). The clasts are variable in size. The deposit shows a grain- to mud-supported texture. At the top of Subunit IVA (Section 173-1068A-15R-5), a few limestone clasts (mudstone) are present. Both clasts and matrix contain calpionellids (*Crassiocollaria*?), which would indicate a deposit age of Tithonian-Berriasian (see Fig. F3A). A hiatus separates these sediments from medium to dark brown pelagic claystones with turbidites (Subunits IIB and IIC). The volumetric proportion of turbidites and pelagites varies from the base of Subunit IIC toward the top. In the deepest part of Subunit IIC, pelagites dominate. Further upcore, from interval 173-1068A-11R-CC to 8R-5, 25 cm, turbidites form >50% of the sediment. Pelagites dominate again from Section 173-1068A-8R-5, 25 cm, up to Sections 4R-5 or 4R-6, and Sections 4R-5 or 4R-6 up to the top of the cored interval (Section 1R-1) are dominated by turbidites (Shipboard Scientific Party, 1998a).

Whereas the pelagic claystones show no visible lithological change throughout Unit II, a significant change in the composition and distribution of the turbidites does occur (Fig. F2). From the Maastrichtian to the Paleocene–Eocene, turbidites are dominated by coarse-grained lithologies, wackestones, grainstones, packstones with grain sizes generally <2 mm, and conglomerates. The coarse-grained sediments often contain shallow-water carbonate particles such as resedimented large foraminifers, bryozoans, algae, reworked shallow-water limestones, and calcarenites (Fig. F3B), but show only a minor terrestrial influence (quartz). Upsection, there is an increasing number of turbidites composed of grains of quartz and mica within a carbonate or clay matrix/cement (calcareous siltstones, clayey siltstones). Throughout the entire sequence, millimeter- to centimeter-thick layers enriched in foraminifers (*Globigerina*) are present (Fig. F3C). Usually they have a sharp base indicating erosion, are well sorted, and have a limited amount of calcareous/clayey matrix. These deposits are most likely formed by the winnowing action of bottom currents (contour currents?).

At distinct levels, characteristic particles occur in the coarse-grained calcareous turbidites. Glauconite can be observed around the Cretaceous/Tertiary boundary and at the Paleocene/Eocene boundary. Small pyrite aggregates and pyrite-filled foraminifers (Globigerinids) also occur at these stratigraphic levels.

Site 1069

The marine sedimentary record at Site 1069 begins with resedimented Upper Jurassic (Tithonian?) shallow-water limestones and minor pelagic/hemipelagic clay (Subunit VA) (Shipboard Scientific Party, 1998b). These sediments, which represent the top of the prerift basement, are draped by an upper Berriasian to lower? Valanginian nannofossil chalk with slump structures in the lower part. A typical texture of these deposits is shown in Figure F3D. The chalk primarily contains fragments of *Inoceramus* shells. A hiatus separates this pelagic carbonate sediment deposited above the CCD from the overlying sub-CCD pelag-

F2. Lithostratigraphic columns for Holes 1068A and 1069A, p. 7.

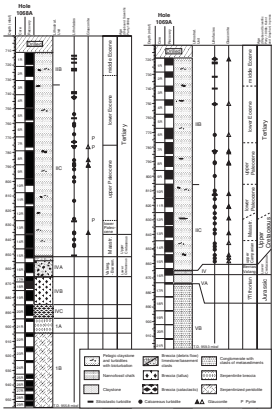

F3. Photomicrographs of samples from Holes 1068A and 1069A, p. 8.

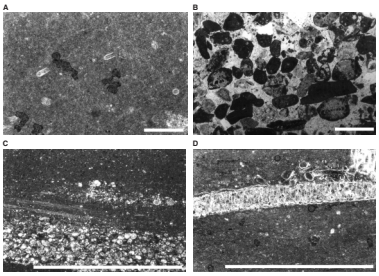

ites of late Campanian to middle Eocene age. This succession is similar to that of Site 1068. The lowermost part of Subunit IIC is dominated by pelagic brown claystones. Turbidites are characteristic for the lower Paleocene sequence (Sections 173-1069A-12R-4, 120 cm, to 9R-1, 125 cm). Pelagites dominate from Section 9R-1, 125 cm, up to 6R-1, 12 cm, whereas turbidites dominate most of the drilled Eocene strata (Section 6R-1, 12 cm, to Core 1R) (Shipboard Scientific Party, 1998b). The composition of turbidites changes successively from calcareous to siliciclastic in the late Paleocene to early Eocene time span. The glauconite distribution is comparable to that at Site 1068 (maximum of particles occurs in the Maastrichtian to lower Paleocene and upper Paleocene–lower Eocene samples) (Fig. **F2**).

SUMMARY

The sedimentary successions at Sites 1068 and 1069 record (syn-?) postrift development on the Iberia Abyssal Plain. The subsidence of possibly 2000–3000 m between the Valanginian and the upper Campanian is shown by the facies change from calcareous pelagic chalk to sub-CCD pelagic claystone on top of the basement highs. In the Upper Cretaceous–lower Tertiary succession, no change in the general lithology is visible and red deep marine claystones form the background sedimentation. However, significant changes occur in the composition of turbidites poured down from the shelf (Galicia Bank). During the early Paleocene to middle Eocene, the dominant carbonate turbidites were successively replaced by quartz/mica turbidites. In the same time interval, and at an earlier stage around the Cretaceous/Tertiary boundary, glauconite occurs in the turbidites. These compositional variations in the turbidites correlate with the presence of palygorskite in the red claystones at the same stratigraphic levels (Wallrabe-Adams et al., 1999).

These variations in sediment and particle input possibly reflect environmental changes on the Iberian shelf (Galicia Bank) induced by sea-level changes related to Paleocene–Eocene global warming (Haq et al., 1987) or tectonic movements in the shelf area connected to the abortive subduction at the southern margin of the Bay of Biscay and Pyrenean orogeny (Boillot et al., 1979). Such events influence the source and distribution of turbidites.

ACKNOWLEDGMENTS

I am grateful for the help and company of both the captain and crew of the *JOIDES Resolution,* as well as of the ODP marine technicians, shipboard scientists, co-chief scientists, and staff scientist. This manuscript has benefited from the careful review and helpful comments of R.N. Hiscott and an anonymous reviewer. I would additionally like to thank ODP for inviting me to participate in Leg 173. J. Welling-Wolf kindly improved the English. Financial support was provided by the Deutsche Forschungsgemeinschaft (grant no. AL 331/4).

REFERENCES

Boillot, G., Auxiètre, J., Dunand, J., Dupeuble, P., and Mauffret, A., 1979. The northwestern Iberian margin: a Cretaceous passive margin deformed during Eocene. *In* Talwani, M., Hay, W., and Ryan, W.B.F. (Eds.), *Deep Drilling Results in the Atlantic Ocean: Continental Margin and Paleoenvironment.* Am. Geophys. Union, Maurice Ewing Ser., 3:138–153.

Haq, B.U., Hardenbol, J., and Vail, P.R., 1987. Chronology of fluctuating sea levels since the Triassic. *Science,* 235:1156–1167.

Kuhnt, W., and Urquhart, E., 2001. Tethyan flysch-type benthic foraminiferal assemblage in the North Atlantic: Cretaceous to Paleogene deep-water agglutinated foraminifers from the Iberia Abyssal Plain (ODP Leg 173). *Rev. Micropaleontol.,* 44:27–59.

ODP Leg 173 Shipboard Scientific Party, 1998. Drilling reveals transition from continental breakup to early magmatic crust. *Eos,* 79:173.

Shipboard Scientific Party, 1998a. Site 1068. *In* Whitmarsh, R.B., Beslier, M.-O., Wallace, P.J., et al., *Proc. ODP, Init. Repts.,* 173: College Station, TX (Ocean Drilling Program), 163–218.

————, 1998b. Site 1069. *In* Whitmarsh, R.B., Beslier, M.-O., Wallace, P.J., et al., *Proc.ODP, Init. Repts.,* 173: College Station, TX (Ocean Drilling Program), 219–263.

Wallrabe-Adams, H.-J., Altenbach, A.V., Kuhnt, W., Pletsch, T., and Schaefer, P., 1999. Facies development of Leg 173 sediments and comparison with tectono-sedimentary sequences of compressional Iberian plate margins. In *Non-volcanic Rifting of Continental Margins: a Comparison of Evidence from Land and Sea: Abstracts of Talks and Posters*. Marine Studies Group/Tectonic Studies Group Discussion Meeting.

Whitmarsh, R.B., Beslier, M.-O., Wallace, P.J., et al., 1998. *Proc. ODP, Init. Repts.,* 173: College Station, TX (Ocean Drilling Program).

Figure F1. Bathymetric chart of the western Iberian margin (contours at 200, 500, 1000, and 1500 through 5500 m). Circles = Leg 149 sites, triangles = Leg 173 sites, solid triangles = Sites 1068 and 1069 as described above. VdG = Vasco da Gama Seamount, VS = Vigo Seamount, PS = Porto Seamount, ES = Estremadura Spur.

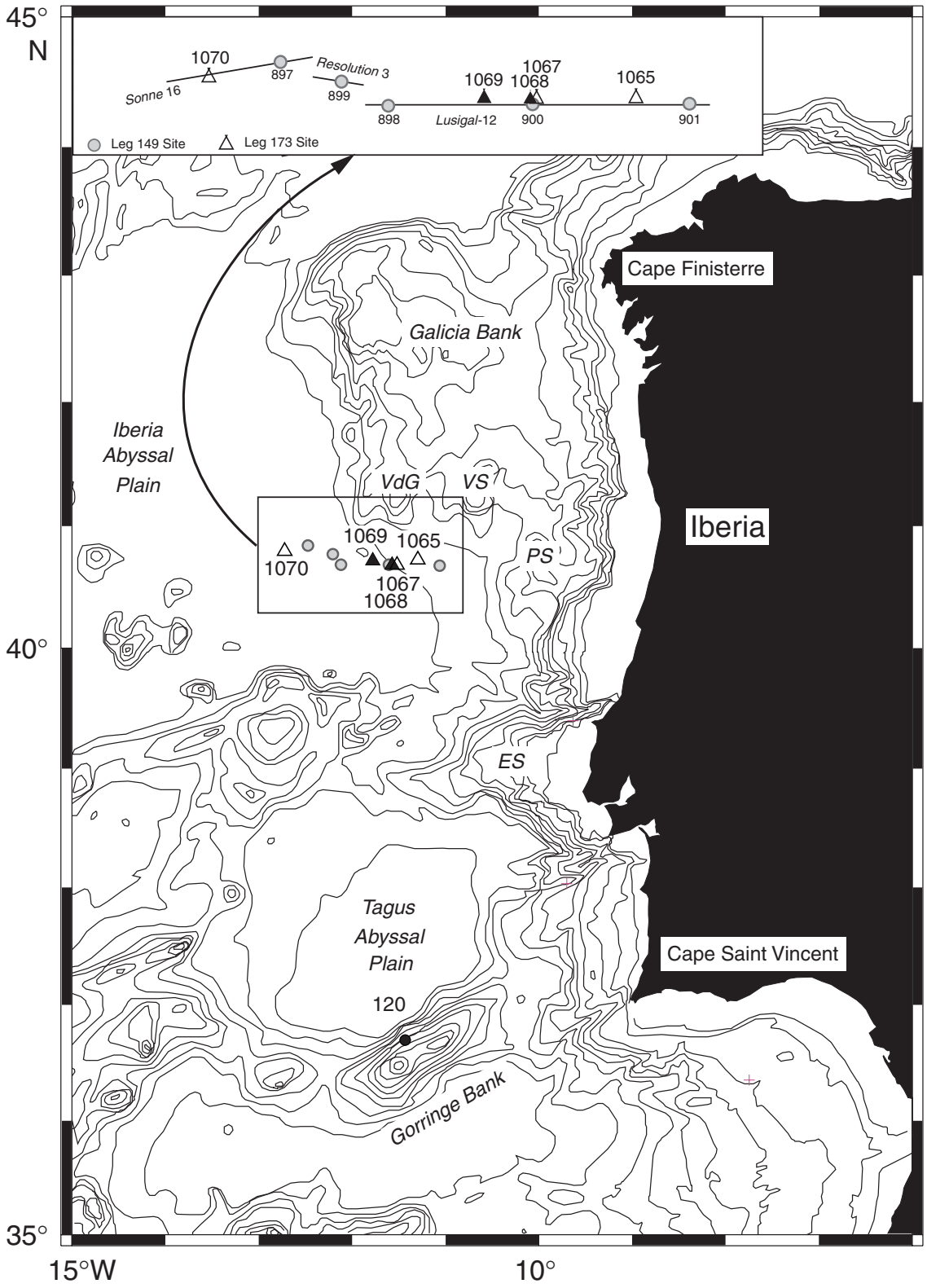

Figure F2. Lithostratigraphic columns for Holes 1068A and 1069A showing the distribution of calcareous coarse turbidites (solid circles) and dominantly siliciclastic turbidites (black bars). Solid triangles = glauconite (open triangles report only trace amounts), P = pyrite.

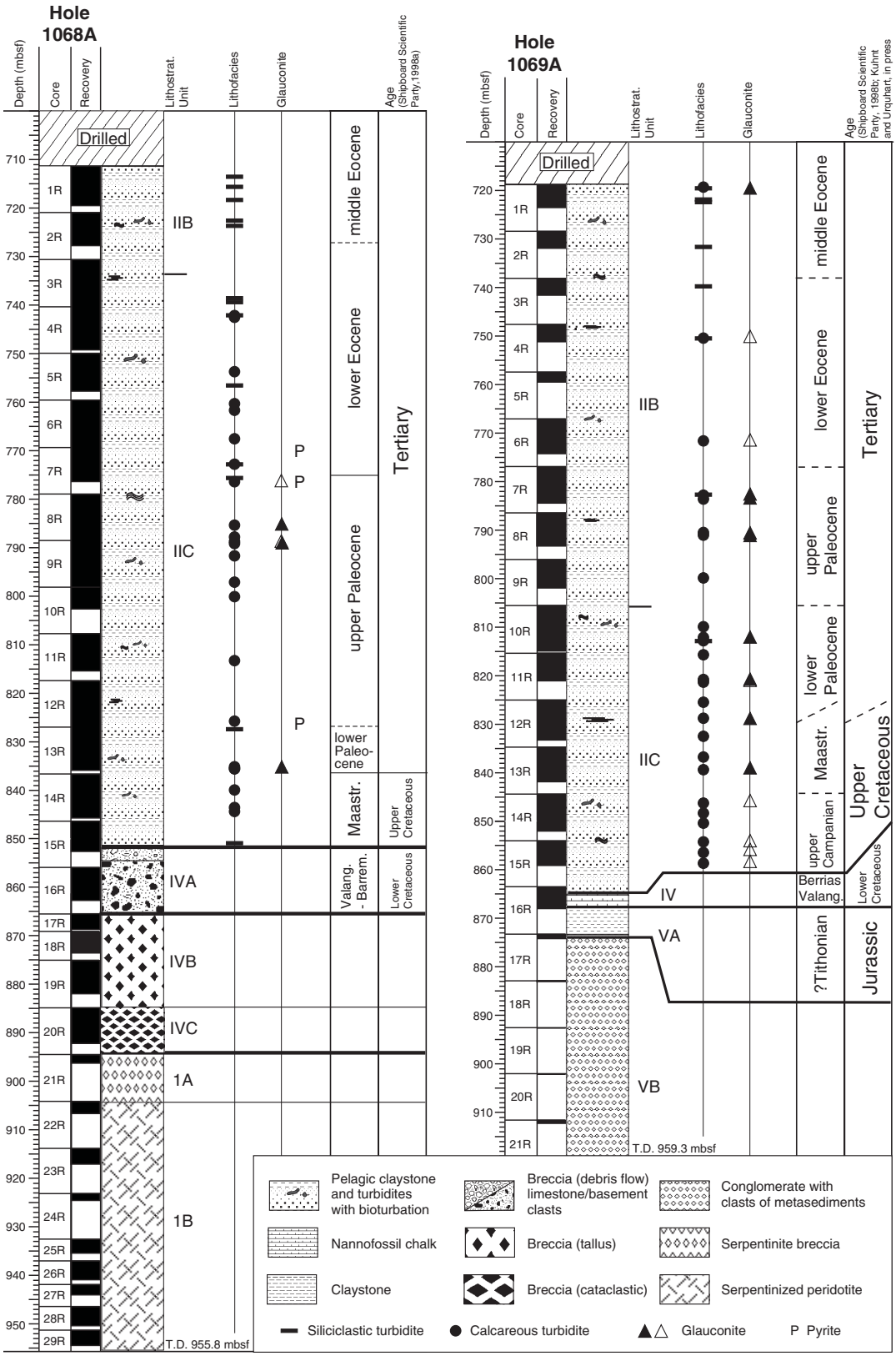

Figure F3. A. Sample 173-1068A-15R-5, 34–35 cm. Calcareous chalk with *Calpionella*. Breccia clast (top of Subunit IVA). **B.** Sample 173-1068A-8R-5, 31–34. Grainstone with limestone clasts and foraminifers (e.g., resedimented *Involutina,* lower right corner). **C.** Sample 173-1068A-6R-1, 53–57 cm. Mudstone with *Globigerina*-wackestone/packstone. Note the sharp basal contact of the *Globigerina* layer. **D.** Sample 173-1069A-16R-2, 45–47 cm. Nannofossil chalk (mudstone) with *Inoceramus* shell. Scale bars = 1 mm.

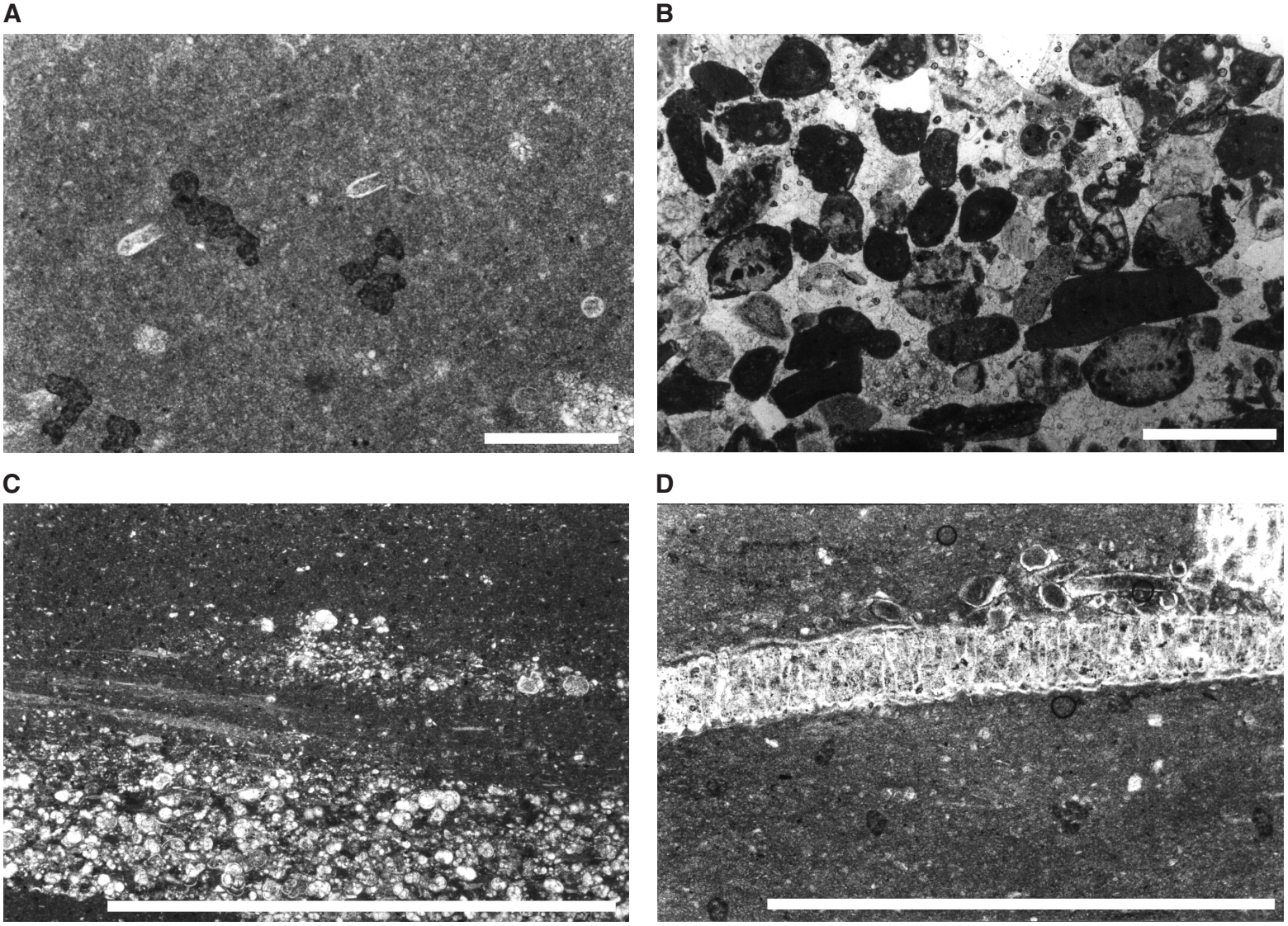

Table T1. Lithology, structure, and significant components of sediment samples, Holes 1068A and 1069A. (See table notes. Continued on next two pages.)

Core, section, interval (cm)	Depth (mbsf)	Age	Lithology	Structure	Glauconite	Terrigenous particles	Remarks
173-1068A-							
1R-2, 102-104	713.82	middle Eocene	Calcareous siltstone	Fine bedding		Quartz, muscovite	Grain supported
1R-4, 1-5	715.81	middle Eocene	Calcareous siltstone/silty claystone	Fine bedding, lamination (wavy)		Quartz, muscovite	Grain supported
1R-5, 92-95	718.22	middle Eocene	Calcareous siltstone/claystone	Fine bedding, wavy lamination		Quartz, muscovite, (plagioclase)	Globigerinids enriched in layers, grain supported
2R-2, 6-9	722.46	middle Eocene	Calcareous siltstone to mudstone	Wavy bedding/lamination		Quartz, muscovite	Grain supported, alignment
2R-2, 127-130	723.67	middle Eocene	Calcareous siltstone to mudstone	Fine bedding, lamination, contorted bedding, bioturbation		Quartz, muscovite	Grain to mud supported, alignment
3R-6, 108-109	738.68	lower Eocene	Calcareous siltstone	Fine bedding, cross bedding		Quartz, muscovite	Globigerinids enriched in clayey layers
3R-7, 20-23	739.30	lower Eocene	Siltstone/claystone/foraminifer sand	Fine bedding, lamination, erosion, bioturbation		Quartz, muscovite; pelite, intraclasts	Peloids
4R-2, 19-21	741.99	lower Eocene	Mudstone with siltstone layers			Muscovite (silt layer: quartz, muscovite, calcite)	
4R-2, 32-35	742.12	lower Eocene	Mudstone-wackestone/siltstone	Lamination		Quartz, muscovite	
4R-2, 47-49	742.27	lower Eocene	Wackestone	Lamination, bioturbation		(Quartz), (muscovite)	Foraminifers filled with sparite
5R-3, 102-105	753.92	lower Eocene	Calcareous sandstone	Lamination, alignment		Quartz, muscovite, plagioclase, calcite	Grain supported
5R-5, 48-49	756.38	lower Eocene	Calcareous siltstone	Lamination		Quartz, muscovite, (plagioclase), calcite	
6R-1, 54-57	760.14	lower Eocene	Mudstone-wackestone, claystone lenses	Lenticular-wavy fine bedding, bioturbation			Foraminifer-rich beds with erosive base
6R-2, 20-24	761.30	lower Eocene	Mudstone/packstone/calcareous siltstone	Fine bedding, lamination, alignments		Quartz, muscovite	Quartz and muscovite in thin beds
6R-6, 24-27	767.34	lower Eocene	Calcareous sandstone	Fine bedding, lamination, alignments		Quartz, (muscovite), (plagioclase)	Erosional surfaces
7R-3, 52-57	772.82	lower Eocene	Mudstone/wackestone	Flaser bedding		Quartz, muscovite, pyroxene	Globigerinids filled with pyrite
7R-5, 48-53	775.78	lower Eocene	Calcareous siltstone/mudstone	Lamination		Quartz, (muscovite)	Globigerinids filled with pyrite
7R-5, 89-92	776.19	lower Eocene	Wackestone/packstone	Indistinct bedding	(X)	(Quartz)	Globigerinids filled with pyrite
8R-5, 31-34	785.21	upper Paleocene	Grainstone with calcareous siltstone	Indistinct bedding, alignment	X	Quartz	Grain supported
8R-6, 140-143	787.80	upper Paleocene	Rudstone/wackestone-packstone/ quartz-bearing mudstone	Fine bedding, lamination, grading, imbrication		Quartz, (muscovite); metapelite	
8R-7, 61-63	788.51	upper Paleocene	Grainstone		(X)	(Quartz)	Grain supported
8R-CC, 8-10	788.61	upper Paleocene	Grainstone		X	Quartz	Grain supported
9R-2, 140-141	791.40	upper Paleocene	Rudstone (conglomerate)			Quartz, muscovite; metapelite, schist, quartzite	Grain supported
9R-6, 100-104	797.00	upper Paleocene	Wackestone with quartz	Lamination, alignment		Quartz	
10R-2, 42-44	800.02	upper Paleocene	Peloidal wackestone/packstone	Lamination, bioturbation		(Quartz)	Peloids ~50%
11R-4, 97-100	813.17	upper Paleocene	Calcareous sandstone	Fine bedding, lamination, cross bedding		Quartz	Grain supported
12R-6, 105-108	825.85	upper Paleocene	Wackestone/packstone to claystone (*)	Fine bedding, lamination, deformation, bioturbation		Quartz	Soft sediment deformation, erosion
13R-1, 12-14	827.02	lower Paleocene	Calcareous siltstone	Fine bedding, erosion surfaces		Quartz	Pyritized foraminifers and pyrite grains
13R-6, 61-63	835.01	lower Paleocene	Wackestone	Indistinct lamination, bioturbation		(Quartz)	Mud supported; top of turbidite
13R-6, 76-78	835.16	lower Paleocene	Wackestone	Fine bedding, lamination, erosion		(Quartz)	Mud supported; center of turbidite
13R-6, 88-91	835.28	lower Paleocene	Packstone	Indistinct lamination, alignment	X	Quartz	Grain supported, solution contacts; base of turbidite

Table T1 (continued).

Core, section, interval (cm)	Depth (mbsf)	Age	Lithology	Structure	Glauconite	Terrigenous particles	Remarks
14R-3, 49-52	840.09	Maastrichtian	Calcareous sandstone	Fine bedding, lamination, bioturbation		Quartz, muscovite, calcite	Grain supported
14R-5, 96-99	843.56	Maastrichtian	Packstone/wackestone	Fine bedding, deformation structures		Quartz, muscovite	
14R-5, 146-149	844.06	Maastrichtian	Packstone/wackestone	Fine bedding, bioturbation		Quartz, muscovite	
15R-4, 84-88	851.14	Maastrichtian	Calcareous siltstone/silty claystone (*)	Fine bedding, bioturbation	(X)	Quartz, muscovite, calcite	
15R-5, 17-23	851.59	Lower Cretaceous	Mudstone-wackestone/calcareous siltstone-claystone.	Convolute bedding, deformation structures		Quartz, muscovite	Contact between mass flow and pelagic series
15R-5, 34-35	851.76	Lower Cretaceous	Mudstone				Clast of mass flow
15R-5, 39-41	851.81	Lower Cretaceous	Mudstone-wackestone				Matrix of mass flow
17R-1, 1-4	865.61	Basement	Breccia with basement clasts				
17R-2, 37-40	867.33	Basement	Breccia with basement clasts				
173-1069A-							
1R-1, 87-90	719.67	middle Eocene	Calcareous siltstone/carbonate sandstone	Layered	X	Quartz	Mud supported
1R-3, 17-21	721.97	middle Eocene	Calcareous siltstone	Fine bedding, lamination		Quartz, muscovite	
1R-3, 28-31	722.08	middle Eocene	Silty claystone (*)	Lamination, bioturbation		Quartz, muscovite	
2R-3, 51-54	731.29	middle Eocene	Calcareous siltstone/mudstone	Fine bedding, lamination		Quartz, (muscovite)	Coarse layers grain supported
2R-3, 78-80	731.56	middle Eocene	Calcareous siltstone-claystone (*)	Fine bedding, lamination		Quartz, muscovite	
3R-2, 26-29	739.86	lower Eocene	Wackestone/calcareous siltstone	Fine bedding, bioturbation		Quartz, muscovite, (plagioclase)	
4R-2, 132-134	750.52	lower Eocene	Calcareous sandstone/silty claystone-clayey siltstone	Fine bedding, lamination, bioturbation	(X)	Quartz, muscovite, (plagioclase), (pyroxene)	
6R-3, 123-124	771.33	lower Eocene	Grainstone		(X)	Quartz, plagioclase; pelites	Grain supported
7R-5, 13-15	782.93	upper Paleocene	Grainstone/calcareous siltstone	Fine bedding, lamination	X	Quartz, (muscovite)	Grain supported
7R-5, 68-70	783.48	upper Paleocene	Grainstone	Fine bedding, lamination	X	Quartz	Grain supported
8R-3, 102-104	790.42	upper Paleocene	Grainstone-rudstone (conglomerate)	Alignment	X	Quartz; pelites	Grain supported
8R-3, 127-130	790.67	upper Paleocene	Calcareous sandstone/siltstone	Fine bedding, lamination	X	Quartz, muscovite	Grain supported
9R-3, 82-83	799.82	upper Paleocene	Grainstone	Fine bedding, lamination		Quartz	Grain supported
9R-3, 86-88	799.86	upper Paleocene	Calcareous siltstone/sandstone	Flaser lamination		Quartz, (muscovite)	
10R- 3, 136-139	809.96	lower Paleocene	Packstone	Fine bedding		Quartz	Grain supported
10R-5, 55-57	812.15	lower Paleocene	Calcareous siltstone/foraminifer-sandstone	Fine bedding (cross/flaser), lamination	X	Quartz, (plagioclase)	Grain supported; top of turbidite
10R-5, 61-64	812.21	lower Paleocene	Grainstone	Fine bedding, lamination		Quartz, (plagioclase)	Grain supported; center of turbidite
10R-5, 69-71	812.29	lower Paleocene	Grainstone			(Quartz), (plagioclase)	Grain supported; base of turbidite
10R-5, 90-93	812.50	lower Paleocene	Grainstone			(Quartz), (plagioclase)	Grain supported
10R-5, 99-103	812.59	lower Paleocene	Calcareous siltstone-claystone (*)	Flaser bedding		Quartz, muscovite	Four fining upward cycles with erosive base
10R-7, 1-4	812.91	lower Paleocene	Grainstone			(Quartz)	Grain supported
11R-1, 65-67	815.95	lower Paleocene	Grainstone-foraminifer sandstone	Graded		(Quartz), (meta-pelites)	Grain supported
11R-4, 95-98	820.75	lower Paleocene	Calcareous siltstone/foraminifer sandstone	Lamination, fine cross bedding	X	Quartz, (muscovite)	Grain supported
11R-CC, 17-20	821.12	lower Paleocene	Grainstone	Lamination	(X)	Quartz	Grain supported
12R-1, 26-29	825.26	lower Paleocene/ Maastrichtian	Grainstone			(Quartz)	Grain supported
12R-3, 98-102	828.98	lower Paleocene/ Maastrichtian	Calcareous siltstone/grainstone	Fine bedding	X	Quartz, (plagioclase), (muscovite)	
12R-6, 11-13	832.61	Maastrichtian	Rudstone (conglomerate)			Quartz; pelite, quartzite	Grain supported
13R-2, 51-54	836.71	Maastrichtian	Rudstone (conglomerate)			Quartz; (pelite)	Grain supported

Table T1 (continued).

Core, section, interval (cm)	Depth (mbsf)	Age	Lithology	Structure	Glauconite	Terrigenous particles	Remarks
13R-3, 146-149	839.16	Maastrichtian	Grainstone	Bedding by grain size	X	Quartz, (muscovite); meta-pelite	
14R-2, 26-29	846.16	upper Campanian	Calcareous siltstone/sandstone	Fine bedding, alignment of elongate particles	(X)	Quartz, muscovite, (plagioclase)	Grain supported
14R-3, 80-84	848.20	upper Campanian	Silty claystone/foraminifer sandstone (*)	Fine bedding		Quartz, (muscovite), (plagioclase)	
14R-4, 133-137	850.23	upper Campanian	Grainstone-rudstone (conglomerate)/ calcareous siltstone	Bedding		Quartz, plagioclase; meta-pelite, schist	Grain supported
15R-1, 21-23	854.21	upper Campanian	Grainstone		(X)	Quartz; pelite	
15R-2, 102-106	856.52	upper Campanian	Grainstone/foraminifer sandstone	Bedding	(X)	Quartz, plagioclase, muscovite; pelite	Grain supported
15R-4, 31-35	858.81	upper Campanian	Calcareous sandstone/grainstone	Graded	(X)	Quartz, plagioclase; meta-pelite, schist	Grain supported
16R-2, 45-47	865.55	Barremian-Valanginian	Mudstone				
16R-2, 93-96	866.03	Barremian-Valanginian	Mudstone	Flaser lamination			
16R-2, 146-149	866.56	Barremian-Valanginian	Mudstone				

Notes: * = samples of pelagic claystone (nonturbidite) or turbidite–pelagite transition. Slash (lithology A/lithology B) = both distinct lithologies occur in the sample; hyphen (lithology A-lithology B) = transitions between lithologies. Components are in order of abundance. X = present, (X) = rare.